16th World Conference on Earthquake, 16WCEE 2017

Santiago Chile, January 9th to 13th 2017

Paper N° 3859

Registration Code: S-S1458535627

INFLUENCE OF LIQUEFACTION AND ADJACENT STRUCTURES ON SEISMIC RESPONSE

G. Barrios [(1)], T. Larkin [(2)], N. Chouw [(3)]

[(1)] *PhD student, The University of Auckland, gbar737@aucklanuni.ac.nz*
[(2)] *Senior Lecturer, The University of Auckland, t.larkin@auckland.ac.nz*
[(3)] *Associate Professor, The University of Auckland, n.chouw@auckland.ac.nz*

Abstract

During past decades the destructive potential and the complexity of soil liquefaction phenomenon associated with strong earthquakes has been widely documented. However, current structural seismic design generally neglects the influence of the subsoil. Design codes that deal with liquefaction usually focus the settlements that can affect the structural foundations. Additionally, most studies related to soil-structure interaction have focused on the response of an isolated structure. In reality, especially in urban areas, this assumption rarely can be justified. The omission of adjacent structures can lead to inaccurate results, especially when nonlinear behaviour of soil, e.g. resulting from liquefaction, takes place. The aim of this work was to implement a holistic approach to the study of liquefaction. The influence of an existing structure on the liquefaction potential will be presented. Also, the effects of adjacent structures on the seismic response will be investigated under conditions of liquefaction. To reach those goals, a series of physical experiments were performed in the centrifuge facilities of the Japanese Institute of Occupational Healthy and Safety (JNIOSH) in Tokyo. A laminar box was used to reduce boundary effects. Rigid blocks were used to represent the influence of a shallow foundation on the underlying soil. In order to achieve a homogeneous density, the sand was rained from a fixed height above the base of the box. Preliminary results show a higher settlement for a stand-alone structure compare with free-field condition. It was found that an adjacent structure had a significant influence of the response of the foundation soil

Keywords: Centrifuge test; Structure-soil-structure interaction; liquefaction; adjacent structures

1 Introduction

Methodologies to deal with high liquefaction risk usually consider the evaluation of settlement and mitigation techniques to reduce it to an "acceptable value". However, this apparently simple approach can lead to several issues. Surface settlement is usually calculated based on estimations of post-shaking volumetric deformation assuming the ground shaking as an undrained event. Recently, Dashti, et al. [1] concluded that most settlement occurs during the earthquake strong shaking, due to partially drained cyclic loading. Also, the authors highlighted that this phenomenon tends to be associated with a structure producing "building-induced" shear deformation in the foundation soil. The influence of a building on the pore-water pressure increment have been previously presented by Rollins and Seed [2] based on field observations. Another issue that is commonly not addressed is the possible effects on the structure due to changes in liquefied soil response (e.g. soil softening). Based on evidence form the 1999 Kocaeli (Turkish) earthquake Sancio et al. [3] remarked that building's settlement is affected by a large number of other variables hard to independently assess. In the numerical field, the recent research by Lopez-Caballero and Modaressi [4] constitutes a significant progress. These authors analysed the possible beneficial or detrimental effect of SFSI. Researchers concluded that the evolution of a pore-water pressure profile is affected by the presence of a structure.

Most methodologies to address soil-foundation-structure interaction consider its effects as mainly beneficial. An overview of different analytical design methods considering SFSI was presented by Stewart et al. [5]. The same year the authors presented a summary of some recommendation based on empirical findings [6]. These beneficial effects were questioned by Mylonakis and Gazetas [7], reaffirming the complexity of the phenomenon. Additionally, when clustered structures are considered, the phenomenon becomes a dynamic cross interaction between the structures and the surrounding soil. The concept of Structure-Soil-Structure Interaction (SSSI) was introduced by Luco and Contesse [8] to address this phenomenon. A complete literature review on the state of art of SSSI was presented by Lou et al. [9] , which highlighted the lack of experimental research. Observations from two instrumented adjacent building during the 1987 Whittier-Narros, California earthquake presented by Celebi ([10, 11]) was one of the first in-situ studies of SSSI. The author concluded that free-field records were influenced by the presence of a building. Also a relationship between SSSI and Rayleigh waves using cross spectra was presented.

The use of centrifuge facilities allows researchers to represent large prototypes with in a reduced model and improved control of the variables compared with full scale or field tests. The work conducted by Trombetta et al. [12] has been one of the most extensive reports of SSSI observations based on centrifuge tests. Also, the work presented by Hayden et al. [13] is one of the latest attempts to improve the understanding of adjacent structures founded on liquefiable soil. Based on two centrifuge tests these authors studied the behaviour of different structural configurations.

The present work describes preliminary results of 3 tests conducted at the Mark II centrifuge facilities of the Japanese National Institute of Occupational Safety and Health (JNIOSH). Technical information about Mark-II can be found in Horii et al. [14]. The tests performed aim to improve the state of knowledge about liquefiable soil under configurations of stand-alone and adjacent structures on shallow foundation. Toyoura sand and a pore fluid consistent with the associated scaling laws were used. A laminar box was used to reduce the boundary effects and simulate lateral soil deformation.

The first test of the set utilised a free-field condition (no structures). The second test considered two shallow footings on the soil surface. Both structures were located at a distance intended to minimize the interaction between the structures. This test investigates soil-foundation-structure interaction (SFSI). Rigid blocks are employed to represent structures and impose a bearing pressure of 70 and 115 kPa on the prototype scale. Finally, a test considering both footings close to each other was performed to study the influence of adjacent structures (SSSI).

2 Methodology

2.1 Scale factors

Table 1 presents some of the scaling factors associated with the centrifuge tests. N is defined as the centrifugal acceleration. For all tests 50 g acceleration was applied.

Table 1. Scale factors for centrifuge test

Quantity	Model/Prototype
Acceleration	N
Density	1
Length	1/N
Stress	1
Strain	1
Time	1/N

Soil grain geometry and density were not scaled. This is substantiated by two main concepts. Firstly, a particle scaling can lead to a change in the soil behaviour (e.g. sand representing gravel or even clay representing sand). Clearly, important problems can arise from this. Secondly, the foundation size was large enough to include a considerable quantity of particles on the contact area, minimizing the effects of particle size. Additionally, a pore fluid with a viscosity 50 times that of water was used to avoid inconsistences between the scaling factor for consolidation and dynamic time. For further details refer to Kutter [15].

All the results presented henceforth are in prototype scale unless otherwise stated.

2.2 Soil properties

Toyoura sand was used for all the tests. The main properties of this sand are presented in Table 2. These parameters were obtained from previous work conducted on the same facilities by Kido [16].

Table 2. Toyoura sand properties

Parameter	Value
ρ_{min}	1.34 [g/cm^3]
ρ_{max}	1.65 [g/cm^3]
ρ_s	2.64 [g/cm^3]
e_{min}	0.61
e_{max}	0.98

2.3 Models characteristics

Two layers of Toyoura sand were utilised in the laminar box. Firstly, a medium-dense layer (Dr = 70%), 50 mm in height was employed. Above the medium-dense soil layer was a 170 mm layer of loose Toyoura sand (Dr = 40%). At the base of the model a 30 mm thick gravel layer was placed. Soil specimens were prepared by air pluviation to obtain a homogeneous density. Fig. 1 shows a schematic of the soil layers. Thicknesses are presented in the model scale. The corresponding prototype dimensions are presented in brackets.

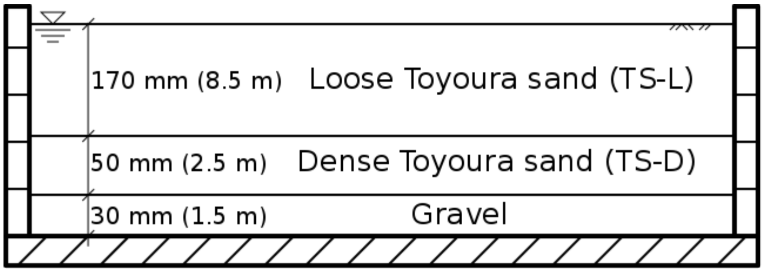

Fig. 1 – Soil specimen cross section

Silicon oil with a dynamic viscosity 50 times that of water was used to saturate the specimen. Due to the high fluid viscosity a vacuum system was used to achieve an adequate saturation level. The vacuum system was composed of four main parts: an air extractor, a safety tank, an oil tank and a vacuum chamber. The air extractor was connected to the safety tank. This safety tank is designed to prevent oil gaining access to the air extraction system. A second tank containing the silicon oil was connected to the safety tank. The oil tank was connected to the vacuum chamber where the sand constituting the specimen was introduced.

The saturation process was conducted in two stages. Firstly, air trapped in the silicon oil and soil specimen was extracted without allowing oil to enter the specimen. An average negative pressure of approximately 100 kPa was applied. Secondly, the oil was allowed to permeate the soil. During this stage a valve in the oil tank was opened a little, otherwise no fluid will enter the soil specimen. A negative pressure of 70 kPa was maintained during this stage.

The soil parameters obtained are presented in Table 3

Table 3. Soil properties

Test	Layer	Description	Height	Density		e	Dr
				Dry	Saturated		
			[m]	[kg/cm^3]	[kg/m^3]		[%]
Free-field	Top	Loose sand	8.5	1.45		0.826	40.5
	Middle	Dense sand	2.5	1.54	$1.91 \cdot 10^8$	0.715	70.5
	Bottom	Gravel	1.5	2.17		0.175	---
SFSI	Top	Loose sand	8.5	1.44		0.831	39.3
	Middle	Dense sand	2.5	1.55	$1.91 \cdot 10^8$	0.707	72.5
	Bottom	Gravel	1.5	2.12		0.205	---
SSSI	Top	Loose sand	8.5	1.45		0.827	40.4
	Middle	Dense sand	2.5	1.53	$1.93 \cdot 10^8$	0.720	69.1
	Bottom	Gravel	1.5	2.12		0.205	---

2.4 Structural models

The main parameters for the structural models were footing dimensions and bearing pressure. The dimensions of the footing were limited by the cross-sectional area (420 mm X 150 mm) of the laminar container. Target bearing pressures were chosen based on a bearing capacity analysis. An analytical study was conducted using the expression presented by Terzagi, Eq. (1).

$$q_f = cN_C + \gamma' D N_q + 0.5\gamma' B N_\gamma \quad (1)$$

The cases studied utilised a cohesionless soil and a surface foundation, thus only the last term of the equation remains. The expression proposed by Loukidis and Salgado [17] was used to evaluate N_γ, Eq. (2). This expression was obtained based on experimental studies using Toyoura sand.

$$N_\gamma = 2.82 \exp\left(\frac{3.64 D_r}{100\%}\right)\left(\frac{\gamma' B}{p_a}\right) \quad (2)$$

The bearing capacity was obtained assuming an angle of internal friction for loose and dense sand of 33° and 39° respectively. These angles of internal friction were obtained based on curves presented by Sanhueza and Villavicencio [18] and are consistent with the work presented by Verdugo and Ishihara [19]. Finally, a bearing capacity of 140 kPa was obtained. Thus, two bearing values of 70 kPa and 115 kPa pressure were selected in the study. These values are close to those employed in engineering design and are close to the soil capacity. Table 4 shows a summary of the properties of the structural models, model dimensions are presented in brackets.

Table 4. Model structural properties

Parameter	Low bearing pressure	High bearing pressure
Width [m]	6.25 (0.125)	6.25 (0.125)
Length [m]	3.5 (0.070)	3.5 (0.070)
Bearing pressure (50 g field) [kPa]	70 (1.41)	115 (2.30)

2.5 General set-up

Instruments in three vertical arrays were used for measurements. Each array consisted of three accelerometers and four pore pressure transducers. Two earth-pressure sensors were located close to surface in the vertical arrays under the footings. Vertical displacement transducers were used to measure surface settlement. Displacement transducers were used to measure lateral displacement of some of the laminar box layers. The location of the different devices considered for the free-field and SFSI tests is presented in Fig. 2. Dimensions are in model scale.

An array was located under the centre line of each footing. The third array was located at the centre of the laminar box. Two displacement transducers were used to measure the vertical movement of each edge of the block. This allows estimation of the settlement and rocking. A displacement transducer was also located at the centre of the specimen. Lateral displacement transducers were placed at surface, 1.5; 3.0; 4.5 and 9.5 m depth (model scale).

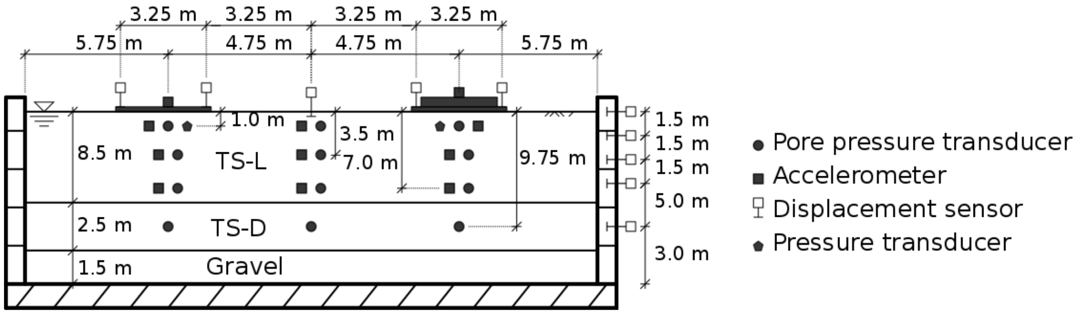

Fig. 2 – Scheme of the devices location

For the SSSI tests the distance, in the direction of shaking, from the edge of the footing to the boundary of the container was approximately equal to the foundation width (B). The distance between footings was close to two times the foundation width (2B). These values were considered suffice to reduce boundary effects from the geometric restrictions of the soil container. The vertical arrays of sensors were place at the same positions for the free-field tests. For the SSSI test the distance between footings was 1.5 m. This distance intended to maximise the interaction between footings and the foundation soil but avoiding pounding between footings. Vertical arrays were located at the centre of the model and beneath the centre line of each footing.

2.6 Ground motions

The motion selected was a harmonic wave with a frequency of 1 Hz (prototype scale). A total of 20 cycles were applied. The first (and last) 4 cycles were a ramp, used to gradually achieve (and decrease from) the maximum amplitude. Maximum accelerations of 0.2 g was considered. Fig. 3 shows the normalized shape of the applied ground motion. Both, model and prototype scales are presented.

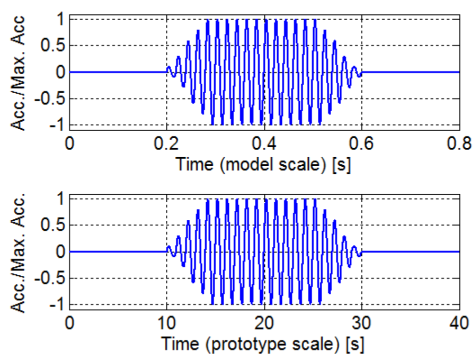

Fig. 3 – Normalized ground motion

3 Free-field test (FF)

The development of the fluid pore pressure recorded by a sensor located at 1 m depth is presented in Fig. 4. As was expected, a monotonic increase (neglecting the high frequency perturbations) of the pore pressure was recorded during the shaking. Fig. 4 also shows the increase in the pore-water ratio r_u (Eq. 3).

$$r_u(z,t) = \frac{\Delta p(z,t)}{\sigma'(z,t=0)} \tag{3}$$

Where $\Delta p(\mathrm{z}, t)$ is the dynamically induced pore pressure, i.e. that in excess of the static value and $\sigma'(\mathrm{z}, t = 0)$ corresponds to the initial vertical effective stress. Therefore, a value of $r_u(t) = 1$ indicates liquefaction triggering. However, the device's progressive settlement was not considered and the vertical effective stress was assumed the same for each test. Therefore, values of $r_u > 1$ were observed (Fig. 4).

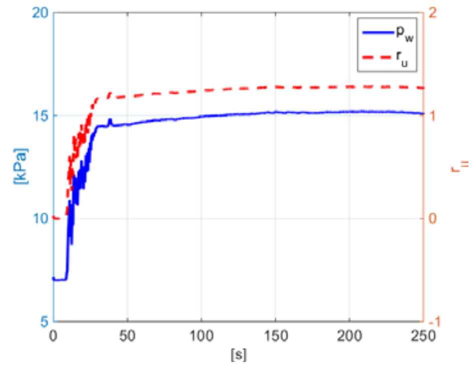

Fig. 4 – Pore fluid pressure

Fig. 5 shows the average of the settlements recorded on the five devices placed on surface. Fig. 5-a shows the settlement observed during the shaking and Fig. 5-b shows the settlement recorded including that occurring post-shaking.

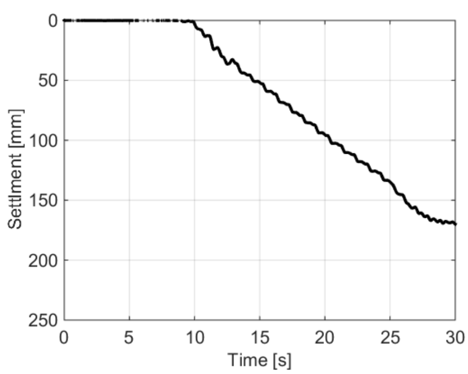

a. Co-shaking settlement

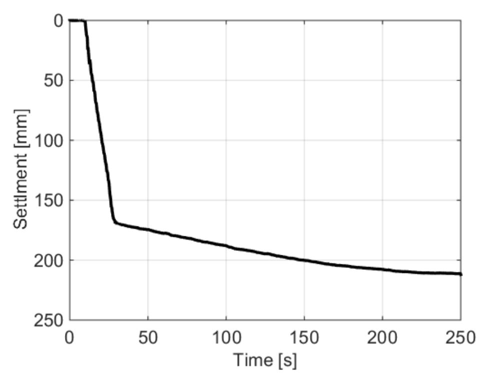

b. Total settlement

Fig. 5 – Average surface settlement

The observed settlement can be divided into two parts. Firstly, that produced during shaking (co-shaking) and, secondly, that after the termination of the shaking (post-shaking). As can be observed in Fig. 5-b the settlements have not achieved a stable value by the end of the record (250 seconds of prototype time). Based on this result, the dynamic recording time was extended to 1000 s for subsequent tests.

4 Stand-alone structures (SFSI)

Two footings with a bearing pressure of 70 and 115 kPa were located at a distance of two times the footing width (see Fig. 2). This distance intended to minimise the interaction between footings.

Fluid pore pressure development with time is shown in Fig 6-a for 1.0 m depth and Fig 6-b for 9.8 m depth. In both figures the pressure beneath the centre of the model is presented in dashed blue line, the record beneath the lower mass in red line and the settlement under the higher mass in dotted black line. Recording from the shallow device (1.0 m) shows a higher pore fluid pressure increment beneath the foundations compared with the centre of the laminar box. At 9.8 m depth (Fig 6-b) the footing's influence seems to disappear.

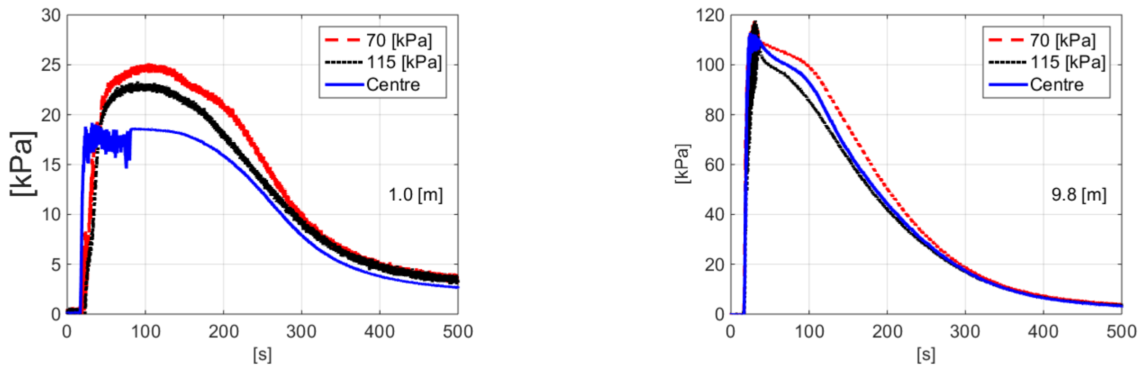

a. 1.0 m depth

b. 9.8 m depth

Fig 6 – Fluid pore pressure at different depths

Fig. 7-a shows the settlement recorded during the test. Two phases can be identified, the component during the shaking and that following the shaking. Fig. 7-b shows the contribution of each component beneath each footing and in the centre of the laminar box. A lower settlement was recorded at the centre. Also, similar co and post-shaking settlement was observed for both footings. However, post-shaking settlement was higher under footings compare with the centre of the specimen.

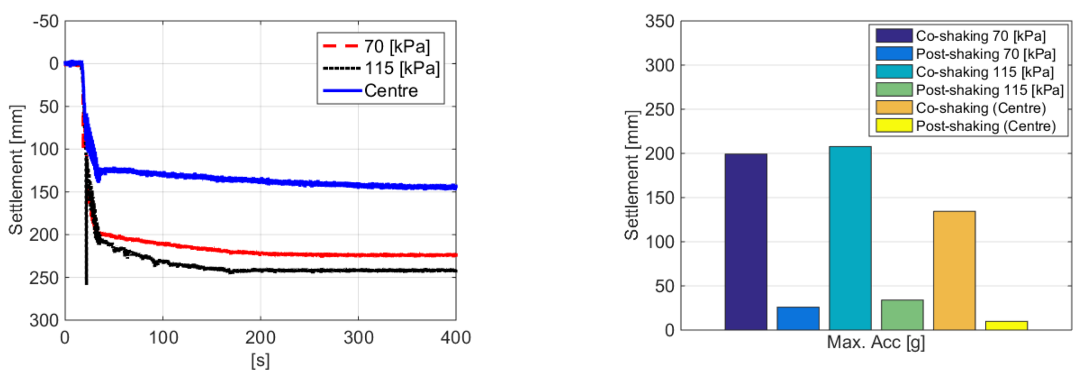

a. Recorded settlement

b. Co and post-seismic contribution

Fig. 7. Average surface settlement (SFSI)

5 Adjacent structures (SSSI)

The same footings considered in the SFSI test were located at 1.5 m apart. This distance was close enough to cause interaction between the footings and the foundation soil (SSSI), but avoiding pounding between them.

Fig. 8-a shows the settlement recorded during the SSSI test. In this test, due to the short distance between the footings, a similar settlement was recorded beneath both footings and at the centre of the laminar box. However, at the centre of the laminar box a slightly lower settlement was observed. Fig. 8-b shows the co and post-shaking components beneath each footing and at the centre of the laminar box.

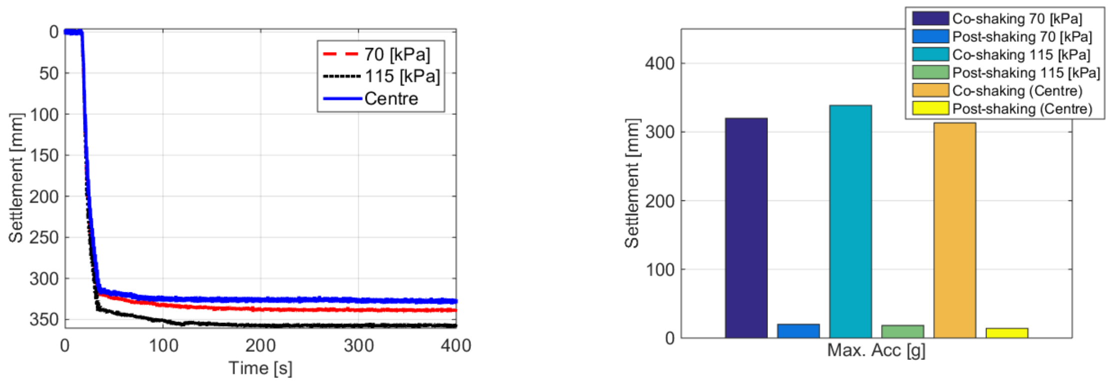

a. Recorded settlement

b. Co and post-shaking contribution

Fig. 8. Surface settlement with interacting masses (SSSI)

Even though the settlement recorded was higher than the SFSI test, it was lower than the sum of settlement of both footings from the SFSI tests. The post-shaking settlement seems to be not affected by the bearing pressure to any marked degree.

6 Conclusions

Preliminary results from three centrifuge tests performed at JNIOSH in Tokyo, Japan are presented. The first test of the set considered a free-field condition. The second test considered two footings with the same contact area but different bearing pressures and the distance between footings was defined to minimize the possible interaction between them. The third test considered the same footings but closely spaced. Observations on vertical settlement, lateral deformation, pore pressure and acceleration were presented. The main conclusions from this works are summarized below.

Free-field condition

- The pore pressure ratio, r_u, can achieve values higher than one due to the device sinking.
- Settlement shows co and post-shaking components.
- The post-shaking component contributes about 25% of the total settlement.

SFSI

- Both footings showed a higher settlement compare with the free-field.
- Regardless of the bearing pressure, a similar settlement was observed on both footings.
- Bearing pressure has a low influence on the post-shaking settlement.

SSSI

- The highest settlement was observed for closely adjacent structures.
- The settlement was lower than the sum of settlement from each footing on the SFSI test.

7 Acknowledgements

The first author would like to thank the Chilean Government for the BECA Chile doctoral scholarship. The authors also wish to thank the NZ Ministry of Business, Innovation and Employment for the financial support through the Natural Hazards Research Platform under the Award UoA 3708936.

8 Copyrights

9 References

[1] S. Dashti, J. D. Bray, J. M. Pestana, M. Riemer and D. Wilson, "Mechanisms of Seismically Induced Settlement of Buildings with Shallow foundations on Liquefiable Soil," *Journal of Geotechnical and Geoenvironmental Engineering,* vol. 136, no. 1, pp. 151-164, 2010.

[2] K. M. Rolins y H. B. Seed, «Influence of builings on potential liquefaction damage,» *Journal of geotechnical engineering,* vol. 116, nº 2, pp. 165-185, 1990.

[3] R. Sancio, J. D. Bray, T. Durgunoglu y A. Onalp, «Performance of buildings over liquefiable ground in Adapazari, Turkey,» de *Proc., 13th World Conf. on Earthquake Engineering*, 2004.

[4] F. Lopez-Caballero y A. Modaressi, «Numerical simulation of liquefaction effects on seismic SSI,» *Soil Dynamics and Earthquake Engineering,* vol. 28, nº 2, pp. 85-98, 2008.

[5] J. P. Stewart, G. L. Fenves y R. B. Seed, «Seismic soil-structure interaction in buildings. I: Analytical methods,» *Journal of Geotechnical and Geoenvironmental Engineering,* vol. 125, nº 1, pp. 38-48, 1999.

[6] J. P. Stewart, R. B. Seed y G. L. Fenves, «Seismic soil-sructure interaction in buildings. II: Empirical findings,» *Journal of Geotechnical and Geoenvironmental Engineering,* vol. 125, nº 1, pp. 26-37, 1999.

[7] G. Mylonakis y G. Gazetas, «Seismic soil-structure interaction: beneficial or detrimental?,» *Journal of Earthquake Engineering,* vol. 4, nº 03, pp. 277-301, 2000.

[8] J. E. Luco y L. Contesse, «Dynamic structure-soil-structure interaction,» *Bulletin of the Seismological Society of America,* vol. 63, nº 4, pp. 1289-1303, 1973.

[9] M. Lou, H. Wang, X. Chen and Y. Zhai, "Structure-soil-structure interaction: literature review," *Soil Dynamics and Earthquake Engineering,* vol. 31, no. 12, pp. 1724-1731, 2011.

[10] M. Celebi, «Seismic responses of two adjacent building. I: Data and analyses,» *Journal of Structural Engineering*, vol. 119, nº 8, pp. 2461-2476, 1993.

[11] M. Celebi, «Seismic responses of two adjacent buildings. II: Interation,» *Journal of Structural Engineering,* vol. 119, nº 8, pp. 2477-2492, 1993.

[12] N. W. Trombetta, H. B. Mason, Z. Chen, T. C. Hutchinson, J. D. Bray and B. L. Kutter, "Nonlinear dynamic foundation and frame structure response observed in geotechnical centrifuge experiments," *Soil Dynamics and Earthquake Engineering,* vol. 50, pp. 117-133, 2013.

[13] C. P. Hayden, J. D. Zupan, J. D. Bray, J. D. Allmond and B. L. Kutter, "Centrifuge Test of Adjacent Mat-Supported Buildings Affected by Liquefaction," *Journal of Geotechnical and Geoenvironmental Engineering,* vol. 141, no. 3, p. 04014118, 2015.

[14] N. Horii, K. Itoh, Y. Toyowasa and Tamate S, "Development of the NIIS Mark-II geotechnical centrifuge," *In Proc. Int. Conf. on Physical Modelling in Geotechnics,* pp. 141-146, 2006.

[15] B. L. Kutter, "Recent advances in centrifuge modeling of seismic shaking," *In Proc. Int. Conf. on Recent Advances in Geotechnical Earthquake Engineering and Soil Dynamics,* pp. 927-941, 1995.

[16] Y. Kido, *Seismic Reinformcement of Pile Foundations by Diaphragm Walls,* Tokyo, 1999.

[17] D. Loukidis and R. Salgado, "Effect of relative density and stress level on the bearing capacity of footings on sands," *Purdue e-Pubs,* pp. 107-119, 2010.

[18] C. Sanhueza and G. Villavicencio, "Estimates of strength parameters from PANDA penetration test and its application to the calculation of bearing capacity and settlement of foundaion soil (1st part)," *Revista de la construcción,* vol. 9, no. 1, pp. 120-131, 2010.

[19] R. Verdugo and K. Ishihara, "The steady state of sandy soils," *Soils and Foundations,* vol. 36, no. 2, pp. 81-91, 1996.